Sonochemical synthesis of amorphous manganese oxide coated on carbon and application to high power battery

Hirokazu Kawaoka, Mitsuhiro Hibino, Haoshen Zhou, Itaru Honma*

*Energy Electronics Institute, National Institute of Advanced Industrial Science and Technology (AIST),
1-1-1 Umezono, Tsukuba, Ibaraki 305-8568, Japan*

Abstract

The nanocomposite material of amorphous manganese oxide and acetylene black (HSMO/AB), was synthesized by sonochemical method. The acetylene black particles were homogeneously coated with amorphous manganese oxide. In order to demonstrate that these characteristic structures were suitable for rapid discharge–charge, the composite material was tested under large current density. The result exhibited 185 mAh g^{-1} in specific discharge capacity under 10 A g^{-1} in current density. Assuming that an operating voltage of 2.5 V, this capacity corresponded 20 kW kg^{-1} in power density and 90 Wh kg^{-1} in energy density.
© 2003 Elsevier B.V. All rights reserved.

1. Introduction

In recent years, energy storage devices with both high energy and high power densities have been vigorously developed for an application to electric vehicles (EVs). The battery properties of ca. 2 kW kg^{-1} of power density and ca. 15 Wh kg^{-1} of energy density are needed for the EV's application in the future [1]. As the electrode materials are basic elements for the battery device, the cathode electrodes should have superior properties to above expected ones. One approach to develop the cathode materials is to enlarge the power density of a lithium secondary battery that has essentially high energy density. Though LiCoO$_2$ used widely as cathode material for the lithium secondary battery has about 140 mAh g^{-1} of available specific capacity, it shows poor performance if it is used on rapid discharge–charge conditions. On the other hand, manganese oxides, which are inexpensive, lightweight, and low-toxic, have been intensively investigated as promising candidate materials against LiCoO$_2$ cathode. Recent investigations [2–7] indicated that some manganese oxides exhibited good rapid discharge performance. Amorphous manganese oxide (HSMO) has been particularly investigated because of its high discharge–charge capacity, which can be attributed

to a valence state change between Mn(III) and Mn(II) in addition to that between Mn(IV) and Mn(III) [6–8].

In order to enlarge power density without reduction of energy density, there are two points to be considered. The first is based on the size and shape of manganese oxide with a view to shortening lithium diffusion length. For particles whose radius is larger than Li diffusion length, the redundant volume where Li$^+$ ion cannot reach will be present in the particle and result in low specific capacity. In particular, the diffusion length of intercalated ion such as Li$^+$ ion in manganese oxide decreases with increasing discharge–charge rate. Hence, an appropriate structure of manganese oxide such as nanosized particles is desirable for high-rate discharge. The second is concerning contact area between manganese oxide and carbon particles which were added for necessity of raising electric conduction due to poor conductivity of manganese oxide. For the high-rate use, the contact area should be enlarged to maintain high electronic conductivity in electrode material. The effective volume for discharge and charge depends on the contribution of the two points described above, the Li diffusion length and the electric conductivity. In fact, synthesis of nanosized amorphous [8] and mesoporous manganese oxides [9] have been investigated for shortening of Li diffusion length. Moreover, it has been reported that composites of micro- or nanosized manganese oxide particles and carbon were produced by co-precipitation to enlarge the contact area between active material and conducting carbon

* Corresponding author. Tel.: +81-298-615648; fax: +81-298-615829.
E-mail address: i.homma@aist.go.jp (I. Honma).

[10–12]. In this report, nanocomposite, where conducting carbon particles were coated homogeneously with thin layer of manganese oxide, was synthesized by wet process for the purpose of reduction of Li diffusion length and enlargement of contact area. There are very few successful results for coating support medium particles in nanoscale by wet process with the materials that had a poor affinity with support media substance, though it has been often reported for substances with affinity. We succeeded to coat carbon particles with metal oxide hydrate by a sonochemical technique.

Sonochemistry has been attracting a great deal of interest because it enables us to synthesize various types of nanosized material and composites [13]. High-intensity ultrasound irradiation to a liquid generates acoustic cavitation [14]. The acoustic cavitation produces reactive radicals from water or other radical sources in aqueous solutions. These reactive radicals often reduce metal ions into metal or metal oxide nanoparticles [15–18]. Various nanocomposites could be also sonochemically synthesized in the presence of support medium, on which nanoparticles were formed [19,20]. However, it has been nanoparticles that were aggregated on support media in almost all of the literatures. Only few researchers [21] reported the fabrication of nanocomposite with homogeneous layer coating structure. The synthesis methods of manganese oxide including Mn(IV) in aqueous solutions are categorized into following three types: the oxidation of Mn^{2+} ion, the reduction of MnO_4^- ion, and the combination of the former two methods ($3Mn^{2+} + 2Mn^{7+} \rightarrow 5Mn^{4+}$). Chen et al. [22] reported the synthesis of colloidal manganese dioxide by sonication to MnO_4^- aqueous solution with surfactants. MnO_4^- ions in the solution were reduced to manganese dioxide nanocrystals about 2 nm in diameter by the radicals derived from surfactants. We report here that nanocomposite of amorphous manganese oxide and carbon with unique structure was fabricated by sonochemical method. Carbon surfaces were coated with amorphous manganese oxide homogeneously and uniformly in nanoscale.

2. Experimental

To prepare the solution exposed to ultrasound irradiation, 1.20 g of $NaMnO_4 \cdot H_2O$ (Aldrich, >97%) was dissolved in 750 ml of deionized water, yielding $0.01 \, mol \, l^{-1}$ solution, and 0.65 g of acetylene black (AB) (Denkikagaku kogyo, DENKA BLACK, $d = 35$ nm, $S = 68 \, m^2 \, g^{-1}$) was added to the solution. The ultrasound (600 W of total power and 100 kHz in frequency) was irradiated to the solution for 6 h in air atmosphere with stirring. A bath-type ultrasound washer (Honda electronics, W-118T) was used to generate ultrasound. No surfactant was used because it may cause some kind of electrochemical side reactions. After sonication, the suspension was filtered and washed several times using deionized water, and then dried at 120 °C in air for 12 h.

Manganese and sodium content in an as-prepared powder were determined by inductively-coupled plasma (ICP) spectrometry. Carbon content was determined from the weight loss after removing manganese oxide in composite powder using a mixture of perchloric acid and phosphoric acid. Scanning electron microscopy (SEM, TOPCON DS-720) was used to roughly observe morphology of composite powder. For observing the contact condition of manganese oxide and carbon, transmission electron microscopy (TEM) were done on Hitachi H-8100, which was attached with Phillips PV9900 for energy dispersive spectrometer (EDS). The size of focused spot of EDS was 5 nm in diameter.

For electrochemical measurements, a three-electrode cell was assembled in argon gas. For working electrode, the composite powder was mixed with 5 wt.% of binder Teflon, ground, and pressed on a nickel mesh (100 mesh). Li metals on nickel mesh were used as counter and reference electrodes. An electrolyte was a $1 \, mol \, l^{-1}$ $LiClO_4$ solution in equal volumes of ethylene carbonate (EC) and dimethyl carbonate (DMC). Galvanostatic discharge–charge was performed between 1.5 and 4.0 V under 0.1, 1, and $10 \, A \, g^{-1}$ in current densities. After each discharge and charge, a circuit was kept open for 30 min.

3. Results and discussion

In 6 h sonication, the color of solution changed into pale from strong purple, obviously indicating that MnO_4^- ions reduced. ICP spectrometry and quantitative chemical analysis revealed that the content of carbon, sodium, and manganese in as-prepared powder were estimated to be 83.03, 0.85, and 9.29 wt.%, respectively. Assuming manganese state to be tetravalent, an empirical formula was determined to be $Na_{0.22}MnO_{2.11} \cdot 0.47H_2O$.

Fig. 1 shows a SEM image of composite powder. The size of particles observed (ca. 35 nm in diameter) was
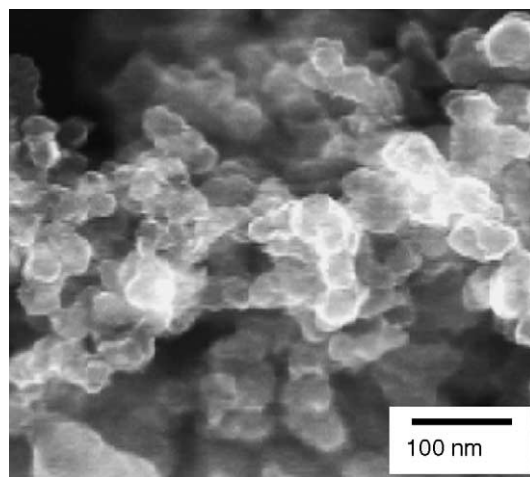

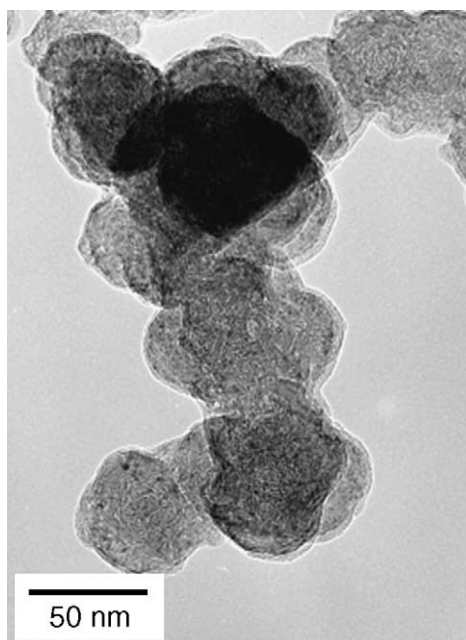Fig. 1. Scanning electron microscopy image of HSMO/AB composite powder.

Fig. 2. Low-resolution transition electron microscopy image of HSMO/AB powder, where AB was coated with amorphous HSMO layer.

approximately the same as that of the AB particles added originally. Manganese oxide particles and their aggregate were not found. TEM observation revealed that a large proportion of AB particles were covered with amorphous substances (Fig. 2). The presence of exposed AB particles was also recognized (not shown here). In other words, not all AB particles were coated with manganese oxide. The thickness of the amorphous substance varied from 1 to 10 nm by particles as shown in Fig. 3a. In order to investigate the composition of amorphous substance, EDS analysis were carried out for the edge (region A) and the interior region of AB (region B), as illustrated in Fig. 3. Carbon, oxygen, sodium, and manganese were detected in the both regions, because the spot size used was larger than the thickness of amorphous layer and because the amorphous substance covered AB for region B. The ratios of peak height of Mn Kα to C K were 0.095 and 0.028 for the regions A and B, respectively. This result shows that manganese concentrated in the amorphous substance. That is the AB particles were coated with the amorphous phase of hydrated sodium manganese oxide, which is abbreviated to HSMO hereafter. The crystalline precipitates embedded in the amorphous phase were also observed in thick regions, though very slightly and not shown in this paper. Fig. 4 shows the powder X-ray diffraction (XRD) patterns for HSMO/AB and AB. In Fig. 4a, there are two broad peaks around 37 and 66° in addition to peaks attributed to AB, indicating the presence of crystalline phases. This is consistent in the TEM observation. Though it was difficult to identify the crystalline phase from only two peaks, it seems that the crystalline phase was thought to be layered birnessite structure, because birnessite-type manganese oxide was preferably formed by sol–gel method
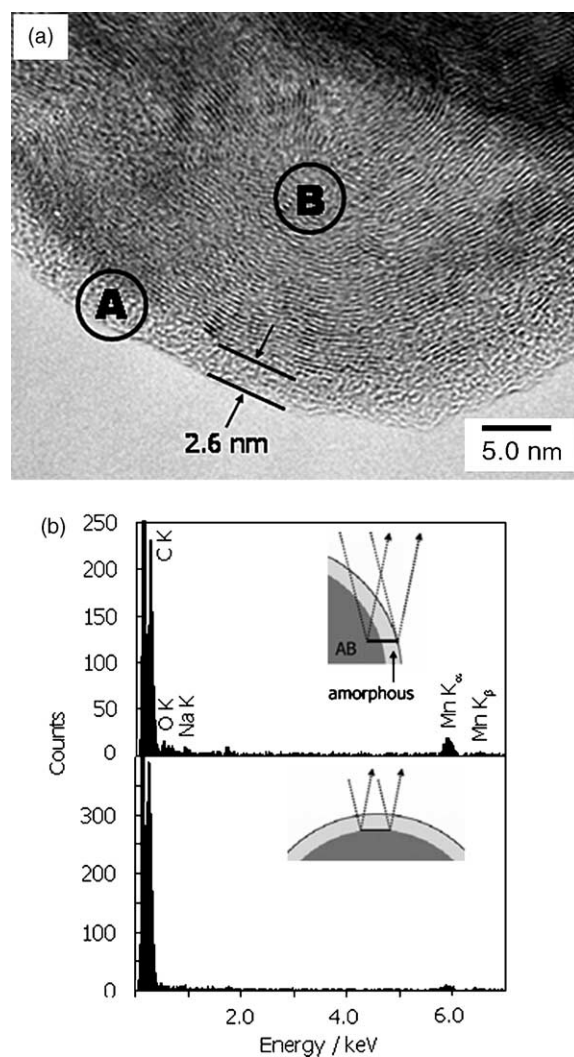

Fig. 3. (a) Transition electron microscopy image of HSMO/AB powder and (b) energy dispersive spectrometer (EDS) analyses with 5 nm in spot size for region A and B.
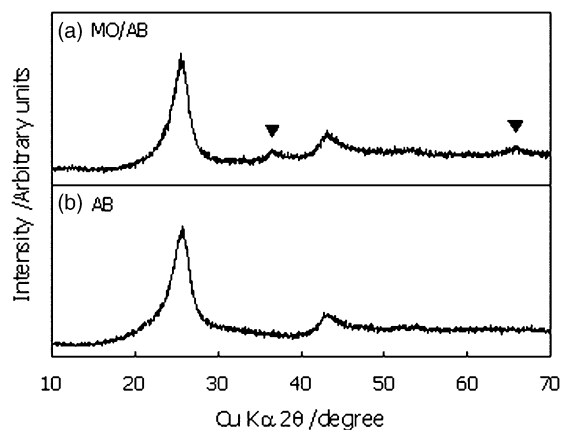

Fig. 4. X-ray powder diffraction patterns of (a) HSMO/AB composite and (b) AB.

in liquid phase [23–27]. Since both of the two observed diffraction peaks are overlaps of multiple ones, we could not estimate crystalline size from width of them.

In almost the sonochemical syntheses of nanocomposites [19,20] previously developed, the reduction occurred by reactive radicals derived from water, alcohol, or surfactant by acoustic cavitation. Support particles introduced in solution were then coated with the nanoparticles pre-produced. In contrast, no source for long-life radical was added in our preparation, and we found that almost no reduction occurred if in the absence of AB. Moreover, in our synthesis the area where MnO_4^- reduced was evidently limited to the surface of AB particles on the grounds that the HSMO covered uniformly the AB and did not form particle consisting from only itself. Pol et al. [21] have demonstrated the similar unique morphology. They fabricated Eu_2O_3/TiO_2 nanocomposite, where TiO_2 particles were coated with amorphous Eu_2O_3 2–5 nm in thick. They proposed that the interparticle collisions between TiO_2 and Eu_2O_3 particles caused by ultrasonic microjets changed the surface reactivity and morphology, which finally resulted in binding or nanolayer coating. In their process, the Eu_2O_3 was formed by hydrolysis of $Eu(NO_3)_3 \cdot 5H_2O$ independently of the presence of TiO_2. In contrast, MnO_4^- ions were not reduced without AB introduction in the present case. Pol's model could not be applied to our case. Though there are possibilities: some sort of reducing agents generated on the surface of the AB particles, or AB surface reduced MnO_4^- catalytically, actual mechanism has not been clarified yet. Further investigations are necessary for establishment of the nucleation and the growth of HSMO layer.

If the AB particles are thoroughly covered with hydrated sodium manganese oxide, the conductivity of composite powder might be markedly reduced, and resulting in a poor cathode performance. Assumed that the density, the thickness of HSMO, and the diameter of AB as $4.0\,g\,cm^{-3}$, 2.0 nm, and 35 nm, 23 wt.% of manganese oxide was required to cover whole AB surfaces. The content of HSMO in the actual composite powder estimated to be 17.0 wt.% from the composition analyses and smaller than the above estimation 23 wt.%. Exposed AB particles in the HSMO/AB were actually observed by TEM as stated above. Consequently, the obtained composite was expected to have enough short distance of lithium diffusion and electron conduction. This implied that the HSMO/AB has a large effective volume for high-rate discharge.

Fig. 5 shows the results of the first discharge to 1.5 V and the charge to 4.0 V using 0.1, 1, and $10\,A\,g^{-1}$ of the current density. These discharge curves had no obvious plateau, and were divided into two regions at about 2.25 V. The region above and below 2.25 V was thought to correspond to change in valence state of manganese from Mn(VI) to Mn(III) and from Mn(III) to Mn(II), respectively [8]. This tendency might be typical for amorphous sodium manganese oxide. For 0.1, 1, and $10\,A\,g^{-1}$, it took 163.8, 12.6, and 1.11 min to discharge 273, 210 and $185\,mAh\,g^{-1}$ in

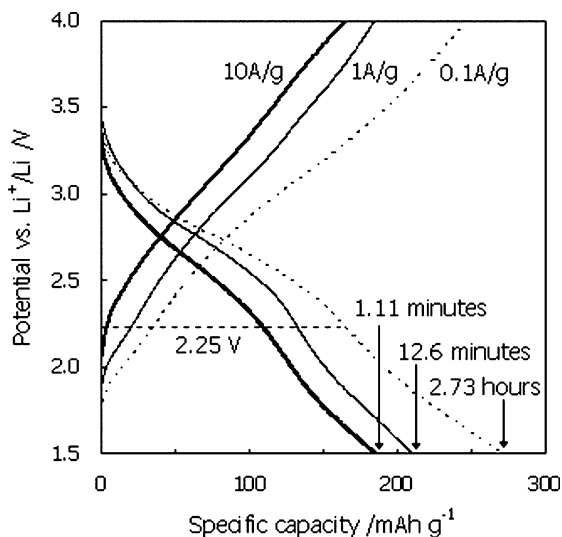Fig. 5. First discharge–charge curves with 0.1 (dotted line), 1.0 (solid line), and $10\,A\,g^{-1}$ (bold line) in current density for HSMO/AB composite.

specific capacity, respectively. Since the discharge capacity of AB powder was $3.3\,mAh\,g^{-1}$ under $0.1\,A\,g^{-1}$, the measured capacities could be attributed to Li intercalation into and extraction from HSMO. The smaller specific capacity for larger current density was observed. This was probably due to a resistance of electrode and a diffusion polarization of lithium. Nevertheless, the level of degradation was so low that large current density could be used for the discharge and charge. This is because the characteristic structure in which the HSMO coated uniformly and thinly on AB allowed high-rate electrochemical reaction. The cycle efficiency (=charge capacity/discharge capacity) was 90, 88, and $90\,mAh\,g^{-1}$ for 0.1, 1, and $10\,A\,g^{-1}$, respectively. Though it was a little apart from unity, it was found that the composite was capable of charging notably fast as well as discharging. The discharge capacity of $273\,mAh\,g^{-1}$ was approximately equivalent to an ideal specific capacity of $LiMnO_2$ ($265\,mAh\,g^{-1}$ for $MnO_2 + Li^+ + e^- \rightarrow LiMnO_2$). Xu et al. [8] have reported $436\,mAh\,g^{-1}$ of discharge capacity for amorphous manganese oxide under $20\,\mu A\,cm^{-2}$ of current density. This was markedly large. They, however, did not investigate about rapid discharge–charge performance. The current density, $1\,A\,g^{-1}$, in the discharge–charge tests in this study corresponded to ca. $20\,mA\,cm^{-2}$ based on our experimental condition. Assuming that an operating voltage of 2.5 V, the result with $10\,A\,g^{-1}$ was calculated to be $20\,kW\,kg^{-1}$ in power density and $90\,Wh\,kg^{-1}$ in energy density, which were much higher than the targeted values [1].

Though, the content of the active material in this nanocomposite was relatively small compared with other general electrode materials in this stage, optimized synthetic conditions will give us the composite containing more HSMO. There is possibility of entire coating of AB surface when the ratio of active material increases. Such structure must reduce electronic conductivity of composite powder.

But we can avoid that if using high surface area carbon, compared to the AB used in this report. It might be better to use the mixture of AB with high surface carbon.

4. Conclusion

The present technique was a simple one for fabricating nanocomposite of amorphous sodium manganese oxide and acetylene black. It was proved that HSMO/AB possessed a unique structure, where the AB particles were uniformly coated with nanosized HSMO layer, and showed satisfactorily high performance of rapid discharge as cathode in lithium ion battery. This synthesis method is expected to enable us to develop lightweight, inexpensive, and low-toxic electrode materials, which can be applied to the power devices requiring both high energy density and high power density.

Acknowledgements

References

[1] R.F. Nelson, J. Power Sources 91 (2000) 2.
[2] M.M. Doeff, A. Anapolsky, L. Edman, T.J. Richardson, L.C. De Jonghe, J. Electrochem. Soc. 148 (2001) A230.
[3] H. Aikiyo, K. Nakane, N. Ogata, T. Ogihara, J. Ceram. Soc. Jpn. 109 (2001) 197.
[4] Y. Shin, A. Manthiram, Electrochem. Solid-State Lett. 6 (2003) A34.
[5] M. Lanz, C. Kormann, H. Steininger, G. Heil, O. Haas, P. Novak, J. Electrochem. Soc. 147 (2000) 3997.
[6] J. Kim, A. Manthiram, Nature 390 (1997) 265.
[7] J. Kim, A. Manthiram, Electrochem. Solid-State Lett. 2 (1999) 55.
[8] J.J. Xu, A.J. Kinser, B.B. Owens, W.H. Smyrl, Electrochem. Solid-State Lett. 1 (1997) 1.
[9] Y.U. Jeong, A. Manthiram, J. Electrochem. Soc. 14 (2002) A1419.
[10] A. Yu, R. Frech, J. Electrochem. Soc. 149 (2002) A99.
[11] M. Hibino, H. Kawaoka, H.S. Zhou, I. Honma, J. Power Sources 124 (2003) 143.
[12] H.Y. Lee, S.W. Kim, H.Y. Lee, Electrochem. Solid-State Lett. 4 (2001) A19.
[13] X. Yang, W. Tang, Z. Liu, Y. Makita, S. Kasaishi, K. Ooi, Electrochem. Solid-State Lett. 5 (2002) A191.
[14] K.S. Suslick, G.J. Price, Annu. Rev. Mater. Sci. 29 (1999) 295.
[15] K.S. Suslick, Science 247 (1990) 1439.
[16] F. Grieser, R. Hobson, J. Sostaric, P. Mulvaney, Ultrasonics 34 (1996) 547.
[17] R.A. Caruso, M.A. Kumar, F. Grieser, Colloids Surf. A: Physicochem. Eng. Asp. 169 (2000) 219.
[18] Y. Mizukoshi, E. Takagi, H. Okuno, R. Oshima, Y. Maeda, Y. Nagata, Ultrason. Sonochem. 8 (2001) 1.
[19] K. Okitsu, Y. Mizukoshi, H. Bandow, Y. Maeda, T. Yamamoto, Y. Nagata, Ultrason. Sonochem. 3 (1996) S249.
[20] K. Okitsu, A. Yue, S. Tanabe, H. Matsumoto, Chem. Mater. 12 (2000) 3006.
[21] V.G. Pol, R. Reisfeld, A. Gedanken, Chem. Mater. 14 (2002) 3920.
[22] W. Chen, W. Cai, Y. Lei, L. Zhang, Mater. Lett. 50 (2001) 53.
[23] T. Fujimoto, Y. Mizukoshi, Y. Nagata, Y. Maeda, Scripta Mater. 44 (2001) 2183.
[24] Y.C. Zhang, H. Wang, B. Wang, H. Yan, A. Ahniyaz, M. Yoshimura, Mater. Res. Bull. 37 (2002) 1411.
[25] M. Tsuda, H. Arai, Y. Sakurai, J. Power Sources 110 (2002) 52.
[26] S. Baffier, J.P. Pereira-Ramos, N. Baffier, J. Electrochem. Soc. 143 (1996) 3429.
[27] J. Cai, J. Liu, S.L. Suib, Chem. Mater. 14 (2002) 2071.